Explorable Data Consistent CT Reconstruction: Supplementary Material

Hannah Dröge[1]
hannah.droege@uni-siegen.de
Yuval Bahat[2]
yuval.bahat@gmail.com
Felix Heide[2]
fheide@cs.princeton.edu
Michael Möller[1]
michael.moeller@uni-siegen.de

[1] Computer Vision Group
University of Siegen
Siegen, Germany

[2] Computational Imaging Lab
Princeton University
Princeton, USA

1 Ablation of Soft Cropping and Transformations

We demonstrate our choice of soft cropping and usage of different transformations in our optimization in Fig. 1 on four samples of our dataset, that all show reconstructions obtained from 100 projection angles. The images in the first column show reconstructions of our full method, i.e. applying transformations T_j and using soft cropping in the optimization process. The images in the middle column of Fig. 1 are obtained without using the transformations T_j and highlight that using transformations can oppress noisy results. The images on the right are created without soft cropping (but with an application of the transformations) and clearly show a hard border around the crop, that could be prevented by using soft cropping.

2 Notations

Table 1 shows the symbols and notations that appear in the paper. Please note that with a slight abuse of notations, we use x and f when referring either to the two-dimensional or to the column-stacked versions of the target image and the recorded sinogram, respectively.

3 Detailed Error Measurements

Table 2 shows the detailed measurements of the error when optimizing malignancy prediction towards a small (0.0) and a large (1.0) value, for the set of originally malignant $S^{\mathcal{M}}$ and originally benign $S^{\mathcal{B}}$ nodules. Furthermore, the standard deviations for the results are listed.

© 2022. The copyright of this document resides with its authors.
It may be distributed unchanged freely in print or electronic forms.

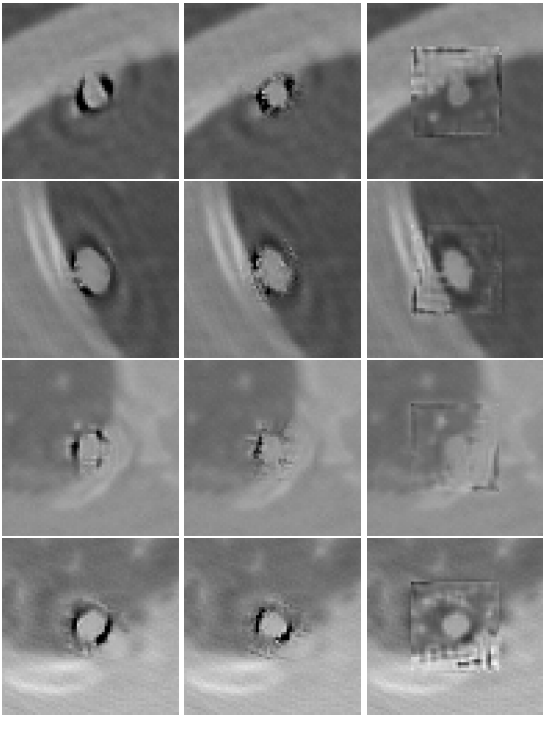

Full method W/o T_j W/o soft cropping

Figure 1: Results for different versions of our method

Symbol	Notation
$x \in \mathbb{R}^N$	tomographic image
$\hat{x} \in \mathbb{R}^N$	solution
$f \in \mathbb{R}^{pd}$	sinogram
$R \in \mathbb{R}^{pd \times N}$	discrete radon transform
$p \in \mathbb{N}$	number of projection angles
$d \in \mathbb{N}$	number of pixels in an one-dimensional X-ray detector
$n \in \mathbb{R}^{pd}$	additive noise
$x_{\mathcal{C}} \in \mathbb{R}^{h \times w}$	tomographic image, cropped to region of interest
$N_\theta : \mathbb{R}^{h \times w} \to [0,1]$	classification network
$m \in [0,1]$	malignancy level
$H_\varepsilon : \mathbb{R} \to \mathbb{R}$	Huber loss (element-wise) $H_\varepsilon(a) = \begin{cases} \frac{1}{2}a^2 & \text{for } \lvert a \rvert \leq \varepsilon, \\ \varepsilon \cdot \left(\lvert a \rvert - \frac{1}{2}\varepsilon \right), & \text{otherwise.} \end{cases}$
$\lambda_1 \in \mathbb{R}$	weighting of the malignancy prediction
$\lambda_2 \in \mathbb{R}$	weighting of total variation regularization
$G \in \mathbb{R}^{h \times w}$	Gaussian mask
$e_i \in \mathbb{R}$	mean squared error of all points in the residual that have an influence on the nodule in the reconstruction
$e_o \in \mathbb{R}$	mean squared error of all points in the residual that don't have an influence on the nodule in the reconstruction
$P \subset \mathbb{R}^N$	solution space of images whose sinogram differs from the measured data by a noise-level dependent constant
$S^{\mathcal{B}} \subset \mathbb{R}^N$	set of reconstructions by filtered backprojection that are classified as benign
$S^{\mathcal{M}} \subset \mathbb{R}^N$	set of reconstructions by filtered backprojection that are classified as malignant

Table 1: Table of notations

	set	p	$\frac{1}{pd}\|Rx-f\|^2 \cdot 10^5$	$N_\theta(x)$	$(e_i - e_o) \cdot 10^5$
optimizing for small N_θ	$S^{\mathcal{B}}$	50	2.56/1.36	0.008/0.009	−1.86/1.08
		100	3.45/2.01	0.015/0.025	0.23/12.82
		200	6.82/3.93	0.048/0.047	22.01/29.92
		360	9.59/5.73	0.067/0.060	52.47/58.06
	$S^{\mathcal{M}}$	50	2.09/1.24	0.003/0.002	−1.50/1.00
		100	3.36/3.48	0.099/0.296	−1.63/2.08
		200	30.16/38.51	0.423/0.375	309.01/461.44
		360	62.15/66.95	0.526/0.395	658.71/801.45
optimizing for large N_θ	$S^{\mathcal{B}}$	50	5.58/2.58	0.960/0.040	−3.73/2.12
		100	3.30/1.76	0.957/0.109	−1.26/1.74
		200	5.82/2.77	0.922/0.168	9.40/18.38
		360	13.45/9.68	0.802/0.286	86.85/98.89
	$S^{\mathcal{M}}$	50	4.55/2.65	0.973/0.031	−2.97/2.22
		100	3.35/3.54	0.986/0.017	−1.83/1.64
		200	2.07/1.71	0.989/0.013	−0.04/3.80
		360	6.55/5.71	0.979/0.026	5.88/15.79
	set	p	$\frac{1}{pd}\|Rx-f\|^2$	$N_\theta(x)$	$(e_i - e_o)$
FBP	$S^{\mathcal{B}} \cup S^{\mathcal{M}}$	50	5.23/9.86	0.54	−1.00/5.43
		100	2.73/8.65	0.55	−1.72/5.34
		200	2.52/8.50	0.55	−1.81/5.32
		360	2.52/8.49	0.55	−1.82/5.31

Table 2: Mean/standard deviation of the data consistency loss, network prediction, and distance between the interior and exterior error $(e_i - e_o)$ of the residual r, for originally benign nodules $x \in S^{\mathcal{B}}$ and malignant nodules $x \in S^{\mathcal{M}}$ optimized towards the most extreme malignancies. For comparison, the last rows of this table show the results of the reconstructions obtained by filtered backprojection.